**The EMBO Journal (2011) 30,** 395–407 | © 2011 European Molecular Biology Organization | All Rights Reserved 0261-4189/11
www.embojournal.org

THE EMBO JOURNAL

# MCL-1 is a stress sensor that regulates autophagy in a developmentally regulated manner

**Marc Germain, Angela P Nguyen, J Nicole Le Grand, Nicole Arbour, Jacqueline L Vanderluit[1], David S Park, Joseph T Opferman[2] and Ruth S Slack***

Department of Cellular and Molecular Medicine, University of Ottawa, Ottawa, Canada

**Apoptosis has an important role during development to regulate cell number. In differentiated cells, however, activation of autophagy has a critical role by enabling cells to remain functional following stress. In this study, we show that the antiapoptotic BCL-2 homologue MCL-1 has a key role in controlling both processes in a developmentally regulated manner. Specifically, MCL-1 degradation is an early event not only following induction of apoptosis, but also under nutrient deprivation conditions where MCL-1 levels regulate activation of autophagy. Furthermore, deletion of MCL-1 in cortical neurons of transgenic mice activates a robust autophagic response. This autophagic response can, however, be converted to apoptosis by either reducing the levels of the autophagy regulator Beclin-1, or by a concomitant activation of BAX. Our results define a pathway whereby MCL-1 has a key role in determining cell fate, by coordinately regulating apoptosis and autophagy.**
*The EMBO Journal* (2011) **30,** 395–407. doi:10.1038/emboj.2010.327; Published online 7 December 2010
*Subject Categories*: differentiation & death; neuroscience
*Keywords*: autophagy; BCL-2 homologues; MCL-1; neurons

## Introduction

Macroautophagy (hereafter referred to as autophagy) is a catabolic process, in which portions of cytoplasm or organelles are delivered to lysosomes for bulk degradation (He and Klionsky, 2009; Mehrpour *et al*, 2010). Autophagy is activated under starvation conditions in order to recycle the nutrients necessary for survival. A basal level of autophagy also exists in nutrient-replete cells to allow the turnover of damaged organelles and long-lived proteins (He and Klionsky, 2009; Mehrpour *et al*, 2010). This basal autophagy is of particular importance in terminally differentiated cells, such as neurons, to prevent accumulation of damaged organelles and proteins (Germain and Slack, 2010). Autophagy has indeed recently been suggested to have a major role in the elimination of protein aggregates associated with several neurodegenerative diseases, such as Alzheimer's and Parkinson's disease. For example, deletion of two important autophagy regulatory proteins (ATG5 and ATG7) in the brain resulted in progressive accumulation of ubiquitin-positive protein aggregates, gradual loss of motor function and death of the animals within a few months of life (Hara *et al*, 2006; Komatsu *et al*, 2006). Several studies have also shown that overexpression of autophagy genes or activation of autophagy by rapamycin leads to a reduction in aggregate formation in models of Alzheimer's, Huntington and Parkinson's disease (Ravikumar *et al*, 2004; Shibata *et al*, 2006; Pickford *et al*, 2008; Spencer *et al*, 2009).

At the molecular level, autophagy is characterised by the formation of a double-membrane vesicle, the autophagosome, containing the material to be degraded (He and Klionsky, 2009; Mehrpour *et al*, 2010). Autophagosomes subsequently fuse with lysosomes for bulk degradation. Autophagosome formation is regulated by a set of autophagy-related (ATG) genes that are conserved from yeast to mammals (Maiuri *et al*, 2007b; He and Klionsky, 2009). Autophagosome nucleation is regulated by a protein complex containing Beclin-1 and the PI3 kinase Vps34, while its elongation requires two ubiquitin-like conjugation systems that are dependent on the activity of ATG7: covalent association between ATG5 and ATG12, and lipidation of LC3 (Maiuri *et al*, 2007b; He and Klionsky, 2009). LC3 lipidation promotes its association with the autophagosome and is widely used as a marker of autophagy.

Apoptosis is a form of cellular suicide required for proper development of multicellular organisms that is controlled by BCL-2 homologues. Antiapoptotic (BCL-2, BCL-$X_L$, A1, MCL-1) and proapoptotic (BAX, BAK) BCL-2 homologues regulate the permeability of the mitochondrial outer membrane. Activation of BH3-only proteins, the third group of BCL-2 homologues, is required for the activation of BAX/BAK, release of cytochrome *c* from the mitochondrial intermembrane space and subsequent activation of caspases, the apoptotic proteases (Youle and Strasser, 2008; Germain and Slack, 2010). In addition to this well-characterised role in controlling apoptosis, BCL-2 homologues have recently been suggested to regulate autophagy (Pattingre *et al*, 2005; Maiuri *et al*, 2007a; Martin *et al*, 2009). For example, BCL-2 and BCL-$X_L$ can both bind to Beclin-1 and inhibit its function (Pattingre *et al*, 2005; Maiuri *et al*, 2007a), although the physiological significance of these interactions has not yet been demonstrated in the context of the whole animal. While there is increasing evidence of an interplay between apoptosis and autophagy (Boya *et al*, 2005; Pattingre *et al*, 2005; Maiuri *et al*, 2007a; Luo and Rubinsztein, 2010), their relative importance in development and adult tissue, as well as the mechanisms by which BCL-2 homologues control the balance between these two cellular fates, remains to be determined.

*Corresponding author. Department of Cellular and Molecular Medicine, Faculty of Medicine, University of Ottawa, 451 Smyth Road, Ottawa, Ontario, Canada K1H 8M5. Tel.: +1 613 562 5800/Ext. 8459; Fax: +1 613 562 5403; E-mail: rslack@uottawa.ca
[1]Present address: Division of Biomedical Sciences, Memorial University, St John's, Newfoundland and Labrador, Canada A1B 3V6
[2]Present address: Department of Biochemistry, St Jude Children's Research Hospital, Memphis, TN 38105, USA

**Received: 26 August 2010; accepted: 16 November 2010; published online: 7 December 2010**

In this study, we used genetic deletion of MCL-1 in post-mitotic neurons to address these questions. We show that apoptosis and autophagy are differentially activated *in vivo* in neural progenitors and post-mitotic neurons, and that MCL-1 degradation lies upstream in a common pathway leading to both cell fates. In fact, a major outcome following MCL-1 degradation is autophagy unless BAX is concomitantly activated or autophagy inhibited, which then induces apoptosis. Altogether, these results indicate that MCL-1 coordinately regulates apoptosis and autophagy, the outcome being determined by the interplay between BAX and Beclin-1 activation downstream of MCL-1 degradation.

## Results

MCL-1 is an antiapoptotic BCL-2 homologue that is rapidly degraded following stress, to allow apoptosis to proceed (Nijhawan *et al*, 2003). More recently, we have shown that MCL-1 is one of the earliest BCL-2 family proteins to respond to stress following acute neuronal injury, before any sign of apoptotic signalling (Arbour *et al*, 2008). Indeed, MCL-1 is degraded following glucose deprivation as a consequence of translation inhibition, and this occurs without signs of apoptosis (Mills *et al*, 2008; Pradelli *et al*, 2010). Here, we confirmed these results in several cell types (Figure 1) and, importantly, extended them to other forms of nutrient deprivation. For example, MCL-1 levels were dramatically decreased upon amino-acid starvation (Figure 1A; cells incubated in Earl's Balanced Salt Solution (EBSS)). Similarly, incubation of cerebellar granule neurons (CGNs) under hypoxic conditions (1% oxygen), or cortical neurons in the absence of glucose, led to a decrease in MCL-1 protein levels (Figure 1B and C), although the faster migrating isoform was decreased in cortical neurons (Figure 1C). Of note, protein levels of other BCL-2 homologues were not affected by nutrient starvation in either cell lines or cortical neurons (Figure 1C), indicating that this effect is specific to MCL-1. In addition, the decrease in MCL-1 protein levels was only transient, as MCL-1 levels returned to normal after reoxygenating hypoxic CGN for 4–8 h (Figure 1B), and within 1 h of re-introduction of glucose to cells that were incubated in glucose-free media for 3 h (Figure 1D), suggesting that MCL-1 degradation is not sufficient to induce apoptosis.

To directly address the consequences of MCL-1 degradation on apoptosis, we analysed the activation of BAX, a proapoptotic BCL-2 homologue that mediates cytochrome *c* release from mitochondria. While MCL-1 levels were reduced following a 3-h incubation of HeLa cells in EBSS (Figure 1E, LacZ), similar to treatment with the apoptotic inducer camptothecin (Figure 1E), no BAX activation (as measured using the conformation-specific antibody 6A7) could be detected in EBSS-treated cells (Figure 1F, LacZ). Accordingly, cytochrome *c* was retained in mitochondria of starved cells (Figure 1G, LacZ), indicating that starvation-induced MCL-1 degradation does not activate the apoptotic cascade. This also suggests that a second, proapoptotic, signal is required to translate MCL-1 degradation into apoptosis. BAX activation is dependent on BH3-only proteins, and both classes of proapoptotic BCL-2 homologues are inhibited by MCL-1. Consequently, MCL-1 degradation (induced by starvation in this case) should enhance BH3-only protein-induced apoptosis. To test this, we infected HeLa cells with an adenovirus encoding the activated form of the BH3-only protein BID (Ad HA-tBID), which directly activates BAX without affecting MCL-1 levels (Figure 1E), in the presence of the pan-caspase inhibitor to prevent cells from lifting following cytochrome *c* release (Germain *et al*, 2005). tBID induced BAX activation and cytochrome *c* release in nutrient-replete cells (Figure 1F and G). However, tBID-induced cytochrome *c* release was greater in starved cells (Figure 1G), despite lower tBID expression (Figure 1E), indicating that BAX activation following nutrient starvation leads to apoptosis. Altogether, these results indicate that MCL-1 levels are highly responsive to nutrient deprivation and that this does not directly result in the activation of apoptosis.

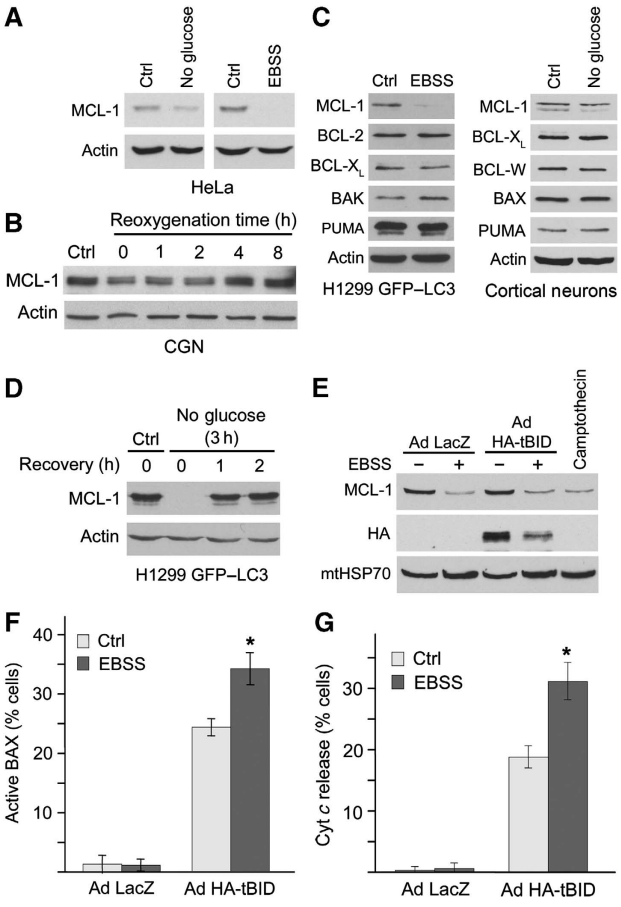


**Figure 1** MCL-1 is degraded following nutrient deprivation. (**A**) HeLa cells were incubated for 4 h in either EBSS or media without glucose/pyruvate. Lysates were then analysed by western blot for the presence of MCL-1, as well as actin as a loading control. (**B**) CGNs were subjected to 17 h hypoxia after 7 days *in vitro*. Protein lysates were collected at indicated times after reoxygenation and blotted for MCL-1 expression and for actin as a loading control. (**C**) H1299 cells stably expressing GFP–LC3 were incubated for 2 h in EBSS, and expression of various BCL-2 homologues was analysed by western blot. Alternatively, primary cortical neurons were incubated for 4 h in media without glucose/pyruvate. (**D**) H1299 cells stably expressing GFP–LC3 were incubated for 3 h in media without glucose/pyruvate, followed by re-addition of glucose and pyruvate for the indicated times. (**E**) HeLa cells were infected with 5 p.f.u. per cell of either Ad HA-tBID or Ad LacZ for 7 h, the media being changed to EBSS for the last 3 h where indicated. Alternatively, cells were treated with 50 μM camptothecin for 3 h. (**F**, **G**) HeLa cells were treated as in **E** in the presence of 50 μM zVAD-FMK and analysed by immunofluorescence for active BAX (6A7 epitope; **F**) or cyt *c* (**G**). Data are expressed as the average of three experiments ± s.d. $^*P<0.01$.

### *MCL-1 is degraded following induction of autophagy*

The results presented above suggest that MCL-1 has a second, apoptosis-independent role in the regulation of cellular stress. A major response activated by nutrient deprivation under conditions that trigger MCL-1 degradation is autophagy. To address the physiological significance of MCL-1 degradation and establish a link between MCL-1 degradation and the induction of autophagy, we analysed the temporal relationship between MCL-1 loss and autophagosome formation. Conversion of a GFP-tagged version of the autophagy marker LC3 (GFP–LC3) from GFP–LC3-I to GFP–LC3-II, its translocation to punctate structures in the cytosol, as well as changes in levels of the LC3-associated protein p62 (which is degraded in the lysosomes under these conditions) have extensively been used to follow autophagy induction in cells. Incubation of H1299 cells stably expressing GFP–LC3 (H1299-LC3) (Chang *et al*, 2010) for up to 8 h in glucose-free media or in EBSS did not cause BAX activation or cytochrome *c* release (Figure 2A and B), but induced loss of p62 protein, processing of GFP–LC3-I into GFP–LC3-II (Figure 2C) and appearance of LC3-positive structures in the cytosol (Figure 2B), indicative of autophagy induction. Under these conditions, loss of MCL-1 protein was an early event, as it occurred before LC3 processing and p62 degradation (Figure 2D).

### *MCL-1 regulates autophagy in cells*

The observation that MCL-1 degradation is associated with activation of autophagy, but occurs before major changes in autophagy markers, suggests that MCL-1 degradation regulates autophagy initiation upstream of autophagosome formation. We took several approaches to test this possibility. First, to assess whether MCL-1 degradation lies upstream of autophagosome formation, MCL-1 levels were measured in the presence of 3-methyladenine (3MA), a class III PI3 kinase inhibitor that blocks autophagosome formation. However, while 3MA caused an increase in p62 levels under both basal and autophagic conditions, reflecting the inhibition of autophagy, it had no effect on MCL-1 degradation (Figure 2E). Similarly, the lysosomal inhibitor bafilomycin blocked p62 degradation, but had no effect on MCL-1 degradation (Figure 2F). Altogether, these results suggest that MCL-1 degradation occurs upstream of autophagosome formation, consistent with a possible regulatory function of MCL-1 in the initiation of autophagy.

We then addressed the function of MCL-1 degradation during autophagy. To preserve MCL-1 levels following induction of autophagy, MCL-1 was overexpressed in H1299-LC3 cells using an adenovirus. Overexpression of MCL-1 decreased the number of GFP–LC3 foci (autophagosomes) (Figure 3A).

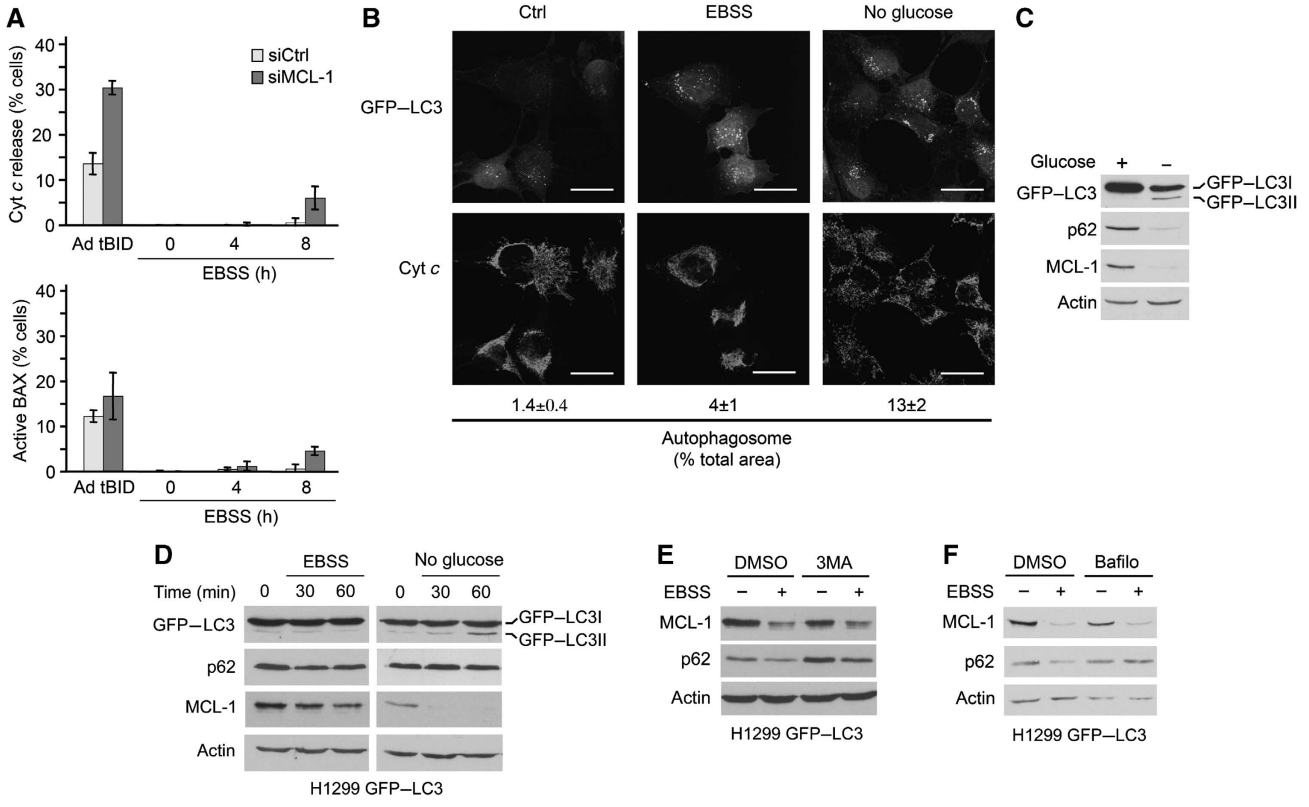


**Figure 2** MCL-1 degradation is an early event following starvation-induced autophagy. (**A**) H1299 cells stably expressing GFP–LC3 were incubated for the indicated times in EBSS in the presence of 50 μM zVAD-FMK and analysed by immunofluorescence for cyt *c* or active BAX (6A7 epitope). As a positive control, cells were infected with 5 p.f.u. per cell Ad HA-tBID for 7 h. Data are expressed as the average of three experiments ± s.d. (**B**) H1299 cells stably expressing GFP–LC3 were incubated for 4 h in either EBSS or media without glucose/pyruvate. Cells were then fixed, stained with an antibody against cyt *c* and analysed by immunofluorescence. Scale bars = 50 μm. Alternatively (**C**), the cells were analysed by western blot for the presence of MCL-1 and the autophagic markers GFP–LC3 (anti-GFP antibody) and p62. (**D**) H1299 cells stably expressing GFP–LC3 were incubated for the indicated times in either EBSS or media without glucose/pyruvate and analysed by western blot for the presence of MCL-1 and autophagic markers. (**E**, **F**) H1299 cells stably expressing GFP–LC3 were pre-incubated for 1 h with 5 mM 3MA (**E**) or 200 nM bafilomycin (**F**), and then incubated for 2 h in complete media or EBSS in the presence of 3MA or bafilomycin. Lysates were then analysed for the presence of MCL-1, the autophagy marker p62 and actin as a loading control.

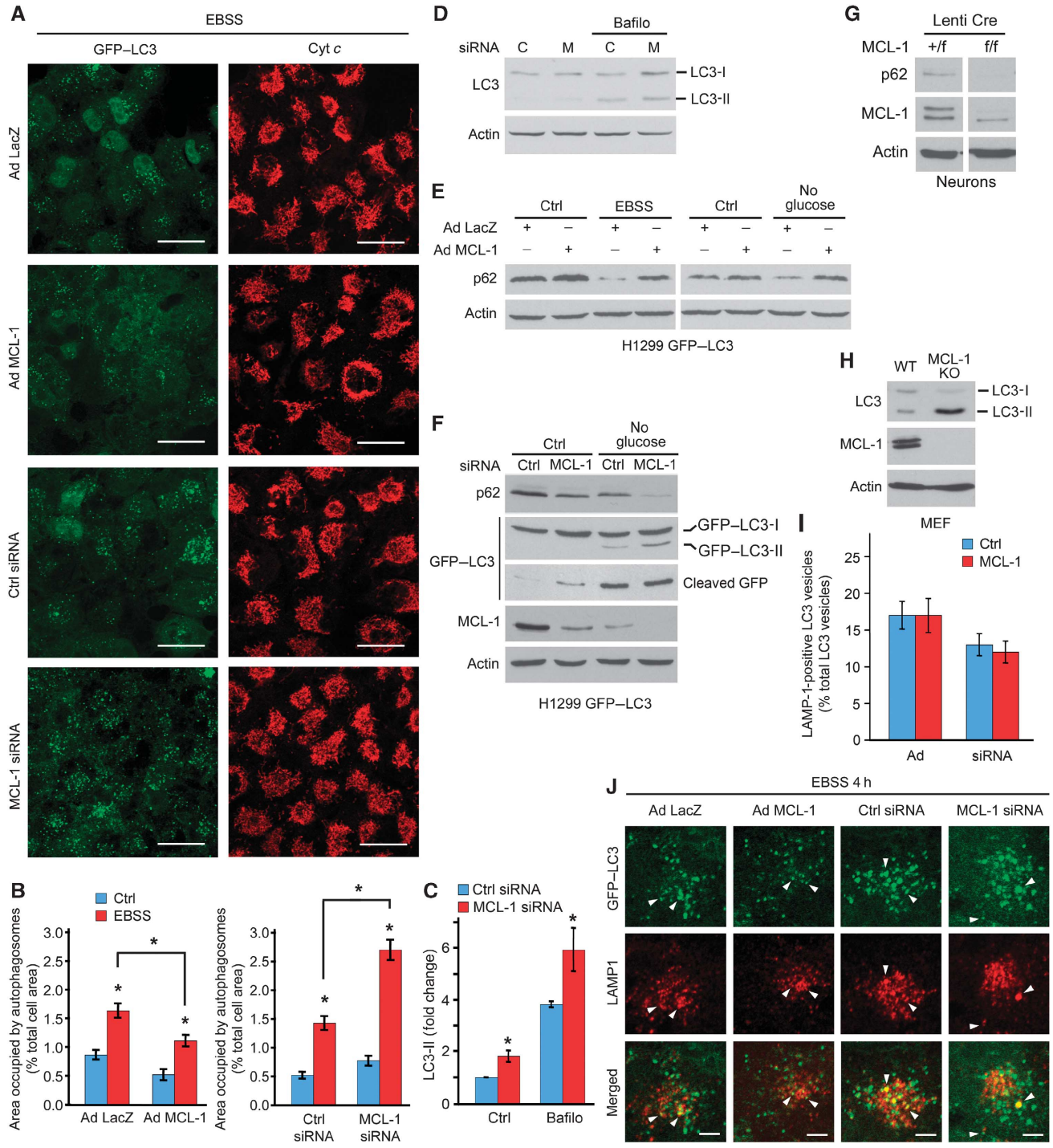


**Figure 3** MCL-1 levels regulate autophagy. (**A**) H1299 cells stably expressing GFP–LC3 were infected with 10 p.f.u. per cell of either Ad LacZ or Ad Myc-MCL-1 for 24 h then incubated in EBSS for 4 h. Alternatively, cells were transfected with control or MCL-1 siRNA 24 h before EBSS treatment. Cells were stained with an antibody against cyt *c* and analysed by immunofluorescence. Representative images are shown. Scale bars = 50 μm. (**B**) The percent of the cell surface area covered by GFP–LC3 vesicles was quantified using the Image J software. $n > 70$ cells in three experiment, $^*P < 0.01$. (**C**, **D**) H1299 cells stably expressing GFP–LC3 were transfected as in **A** and incubated with 200 nM bafilomycin for 1 h where indicated. The levels of endogenous LC3-II relative to actin were quantified by western blot in **C**. Data are expressed as the average of three experiments ± s.d, $^*P < 0.05$. (**E**, **F**) H1299 cells stably expressing GFP–LC3 were treated as in **A** and analysed by western blot for the presence of p62 and GFP–LC3. (**G**) Primary cortical neurons of the indicated genotypes were infected with a lentivirus expressing Cre at the time of plating and analysed for the presence of MCL-1 and p62 by western blot 3 days later. (**H**) Transformed wild-type (WT) and MCL-$1^{\Delta/\Delta}$ (KO) MEFs were analysed by western blot for the expression of endogenous LC3. (**I**, **J**) Colocalization of GFP–LC3 vesicles with the lysosomal marker LAMP1 was analysed by immunofluorescence in cells treated as in **A**. The number of LC3-positive vesicles that colocalised with LAMP1 was quantified in **I**. Data are expressed as the percentage of LC3 vesicles per cell that are LAMP1-positive ± s.e.m., with at least 14 cells per condition. Representative images are shown in **J**. Arrows indicate LC3-positive vesicles colocalizing with LAMP1. Scale bars = 10 μm.

The total surface area occupied by GFP–LC3 vesicles was also quantified, showing a significant decrease in vesicle formation in MCL-1-overexpressing cells (Figure 3B). Cells overexpressing MCL-1 also had increased basal levels of p62, while p62 degradation was reduced in Ad MCL-1-starved cells compared with control infection (Ad LacZ; Figure 3E). These results indicate that increased MCL-1 levels block autophagy.

As these experiments were consistent with an inhibitory role of MCL-1 on the initiation of autophagy, we tested the effect of MCL-1 loss on the autophagic response. Compared with control siRNA, MCL-1 levels were decreased by ~70% in cells transfected with MCL-1 siRNA (Figure 3F). Downregulation of MCL-1 greatly increased the formation of GFP–LC3-positive vesicles (Figure 3A and B), as well as the lipidation of endogenous LC3 (Figure 3C and D). In addition, MCL-1 knockdown resulted in a 50% decrease in p62 levels in cells grown in complete media and a further decrease when cells were grown in glucose-free media for 3 h (Figure 3F). Similarly, MCL-1 knockdown increased processing of GFP–LC3I to GFP–LC3II following starvation, and also caused the accumulation of cleaved GFP (generated through lysosomal degradation of GFP–LC3; Klionsky *et al*, 2008) even in nutrient-replete cells (Figure 3F). Of note, none of these manipulations caused cytochrome *c* release or BAX activation for up to 4 h (Figures 2A and 3A), although some activation of apoptosis was observed at later time points (<10% of the cells at 8h; Figure 2A) when MCL-1 was acutely depleted before starvation rather than as a normal consequence of starvation. Altogether, these results support the conclusion that loss of MCL-1 is not sufficient to induce apoptosis even under starvation conditions.

The role of MCL-1 in the regulation of autophagy was also studied in primary cortical neurons from MCL-$1^{flox/flox}$ animals, in which MCL-1 was removed *in vitro* using a lentiviral vector expressing the Cre recombinase. Consistent with the siRNA results, ablation of MCL-1 in primary neurons caused a marked decrease in p62 levels (Figure 3G). Similarly, an increase in endogenous LC3-II was observed in SV40-transformed MCL-1-null MEFs (Figure 3H). Taken together, these results indicate that MCL-1 negatively regulates autophagy, and that its degradation is required for autophagy to proceed.

One potential explanation for the increase in autophagosomes observed following loss of MCL-1 is the failure of autophagosome fusion with lysosomes, thus resulting in their accumulation. To test this possibility, we further studied the effect of MCL-1 on the fusion between GFP–LC3 vesicles and lysosomes. A fraction of GFP–LC3 vesicles colocalised with the lysosomal marker LAMP1 in EBSS-treated control cells and the percentage of GFP–LC3 vesicles that colocalised with LAMP1 was not affected by overexpression or downregulation of MCL-1 (Figure 3J; quantified in Figure 3I), indicating that MCL-1 does not affect the fusion between autophagosomes and lysosomes. Accordingly, inhibition of lysosomal function with bafilomycin increased endogenous LC3-II levels in both control and MCL-1 knockdown cells (Figure 3C and D). This is consistent with the accumulation of cleaved GFP observed following MCL-1 downregulation. These findings, together with the observation that MCL-1 degradation is upstream of autophagosome formation, suggest that MCL-1 serves as an early regulator of autophagy in cells exposed to nutrient deprivation, its effects being proportional to the strength of the autophagic stimulus.

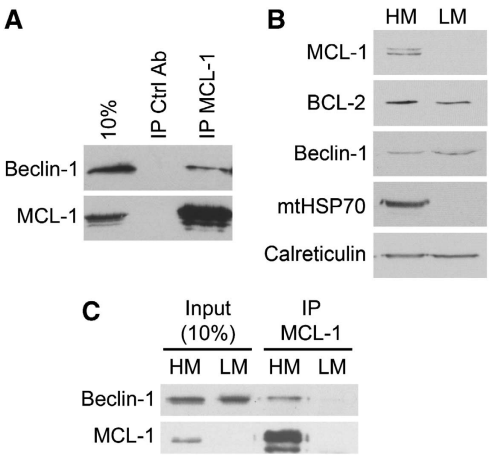


**Figure 4** MCL-1 interacts with Beclin-1 at the mitochondria. (**A**) MCL-1 interacts with Beclin-1. Lysates from H1299 stably expressing GFP–LC3 were immunoprecipitated using control or MCL-1-specific antibodies and analysed for the presence of Beclin-1 by western blot. (**B**) H1299 cells stably expressing GFP–LC3 were fractionated into HM (containing mitochondria), and LM (containing ER). Fractions were analysed for the presence of MCL-1, BCL-2, Beclin-1, the mitochondrial marker mtHSP70 and the ER marker calreticulin. (**C**) MCL-1 was immunoprecipitated from HM and LM before analysing the presence of MCL-1 and Beclin-1.

BCL-2 and BCL-$X_L$ inhibit autophagy by blocking the function of Beclin-1 (Pattingre *et al*, 2005; Maiuri *et al*, 2007a), a key upstream regulator of autophagy (He and Klionsky, 2009). MCL-1 was also reported to interact with GST-tagged Beclin-1 (Erlich *et al*, 2007), an observation that we have extended to the endogenous proteins (Figure 4A). This, along with the observation that MCL-1 inhibits autophagy caused by overexpression of Beclin-1 (Maiuri *et al*, 2007a), suggests that, similar to BCL-2 and BCL-$X_L$, MCL-1 regulates autophagy at least in part by controlling the activity of Beclin-1. Interestingly, while the functional interaction between BCL-2 and Beclin-1 occurs at the endoplasmic reticulum, where both proteins partially localise (Pattingre *et al*, 2005) (Figure 4B), MCL-1 is absent from this organelle (Figure 4B). Rather, MCL-1 is a mitochondrial protein (Chou *et al*, 2006; Germain and Duronio, 2007) in which Beclin-1 also partially localises (Figure 4B) (Pattingre *et al*, 2005; Maiuri *et al*, 2007a), suggesting that MCL-1 interacts with Beclin-1 on mitochondria. To directly test this possibility, cells were fractionated into HM containing mitochondria and LM containing ER, and MCL-1 was immunoprecipitated. As shown in Figure 4C, Beclin-1 co-precipitated with MCL-1 only in the fraction containing mitochondria, indicating that the two proteins interact at the mitochondria and not the ER.

### *Neuron-specific deletion of MCL-1 deregulates activation of autophagy*

At the level of the organism, previous studies have indicated that autophagy has an important role in the homeostasis of the central nervous system (CNS). For example, deletion of key autophagy regulators (ATG5, ATG7) in the CNS leads to progressive accumulation of ubiquitin-containing aggregates and neurodegeneration (Hara *et al*, 2006; Komatsu *et al*, 2006), whereas deletion of Ambra1, a component of the Beclin-1/Vps34 complex, causes major neural tube defects (Fimia *et al*, 2007). To determine whether MCL-1 regulates

autophagy in the CNS, we examined the consequences of MCL-1 deletion in post-mitotic cortical neurons. Mice homozygous for a floxed MCL-1 allele (MCL-$1^{flox/flox}$) were crossed with animals carrying a CamKIIα Cre transgene, resulting in the expression of the Cre recombinase in neurons of the cortex, hippocampus and, to a lesser extent, striatum (Casanova *et al*, 2001). MCL-$1^{\Delta/\Delta}$ mice were born at the expected ratio, but were smaller in size (Figure 5A) and had a median lifespan of 49 days, with a few animals surviving to 3 months (see Figure 8E). Recombination of the floxed alleles was confirmed by western blot of tissue from the cortex of P14 animals (Figure 5B). No change in protein expression was observed for BAX and BCL-$X_L$ (Figure 5B), suggesting that there were little compensatory changes in these other BCL-2 homologues highly expressed in the brain. Cresyl violet staining of brain sections revealed progressive cellular loss in cortical layers adjacent to the corpus callosum in MCL-$1^{\Delta/\Delta}$ animals, with extensive loss evident by P14 (Figure 5C). As we hypothesised that MCL-1 loss would result in increased autophagy, we measured several autophagic markers in MCL-$1^{\Delta/\Delta}$ mice. Brain sections from control and MCL-$1^{\Delta/\Delta}$ mice were stained for endogenous LC3, which appears as punctate staining in the cytosol of autophagic cells. As shown in Figure 5E, LC3-positive cells lined the cortical region where cell loss was observed in P14 MCL-$1^{\Delta/\Delta}$ animals, while minimal staining was present in control mice. Higher magnification images of the affected region confirmed punctate LC3 staining in cells of mutant, but not control animals (Figure 5G; quantification in Figure 5D). Co-staining with the neuronal marker NeuN confirmed that neurons, but not glia, were affected (Figure 5H). To further substantiate these results, the cortex of P14 control and MCL-$1^{\Delta/\Delta}$ mice was examined by electron microscopy. Compared with control, multiple vesicles containing portions of cytoplasm, including mitochondria, were present in the cortex of MCL-$1^{\Delta/\Delta}$ mice (Figure 5F and I; asterisks denote autophagosomal structures; arrows denote mitochondria). These structures were delineated by a double membrane, indicative of autophagosomes (Figure 5I, arrowheads point to the double membrane). As accumulation of autophagosomes could reflect a decrease in their clearance, we also determined p62 levels in MCL-$1^{\Delta/\Delta}$ brains as a measure of lysosomal degradation of autophagosomes. As shown in Figure 6A, p62 levels were decreased in MCL-$1^{\Delta/\Delta}$ cortical extracts, suggesting that loss of MCL-1 does not prevent lysosomal degradation of the autophagosomes. Altogether, these results indicate that the deletion of MCL-1 in cortical neurons results in the deregulated activation of autophagy.

In addition to its role in the regulation of autophagy, MCL-1 has a well-characterised antiapoptotic role during development, including in the CNS (Opferman *et al*, 2003, 2005; Arbour *et al*, 2008). To determine whether MCL-1 has a similarly important antiapoptotic role in post-mitotic neurons, we analysed MCL-$1^{\Delta/\Delta}$ mice for the presence of apoptotic markers. The activated form of BAX (6A7-reactive) and caspase-3 were first detected at P7 in MCL-$1^{\Delta/\Delta}$ mice and were increased by P14 (Figure 6B), suggesting that apoptosis is activated to some extent in these animals. To determine the relationship between autophagy and apoptosis activation, we further analysed BAX activation in relation to LC3 staining. In P7 MCL-$1^{\Delta/\Delta}$ mice, virtually all (97 ± 3%) NeuN-positive neurons were also positive for LC3 (Figure 5H), while only 18 ± 5% of the cells were positive for active BAX (Figure 6B). These BAX-positive cells are neurons with activated autophagy, as they co-stained with LC3 (Figure 6C). In addition, while there are no new cortical neurons generated after birth, the number of LC3-positive neurons decreased at P14 compared with P7 with a concomitant increase in both active BAX and active caspase-3-positive cells that paralleled cellular loss. This suggests that a subset of the neurons that initially activate autophagy in response to MCL-1 deletion undergo apoptosis over time, although we cannot exclude the possibility that apoptosis and autophagy are concomitantly activated in this subset of neurons. Nevertheless, the idea that autophagic MCL-1 KO neurons eventually activate apoptosis is supported by the observation that while all BAX-positive cells were also positive for LC3 at P7, a portion of these cells (8%) was LC3-negative by P14 (Figure 6C; quantification in Figure 8D), in accordance with the notion that apoptosis can inhibit autophagy (Luo and Rubinsztein, 2010).

To further examine the effect of MCL-1 loss on apoptosis in post-mitotic neurons in a system where dying cells are more readily tractable, we deleted MCL-1 from MCL-$1^{flox/flox}$ neurons in culture, which activates an autophagic response (Figure 3G), and analysed the cells for the presence of apoptotic markers. There was no increase in apoptosis in MCL-1 knockout neurons compared with control neurons for up to 10 days in culture, as determined by caspase-3-dependent cleavage of $p130^{CAS}$ into a 31 kDa fragment (Kook *et al*, 2000) (Figure 6D) and cytochrome *c* release (Figure 6E). Altogether, these results suggest that the primary cellular response to MCL-1 deletion in neurons is the induction of autophagy, consistent with our results in cell lines (Figures 1–3).

### *Regulation of apoptosis and autophagy by MCL-1 is dependent on the developmental stage in the CNS*

We previously reported an increase in apoptosis when MCL-1 was deleted in neuronal progenitors (using Foxg1 and Nestin Cre promoters), both *in vivo* and in neural progenitor cultures (Arbour *et al*, 2008). This suggests that the cellular context dictates the final outcome following degradation of MCL-1. To test this possibility, we first examined whether Foxg1-MCL-$1^{\Delta/\Delta}$ embryos (deletion of MCL-1 in neural progenitors) also showed increased autophagy. In contrast to CamKIIα-MCL-$1^{\Delta/\Delta}$ animals (Figure 6A), active caspase-3 was readily detected by western blot in E12.5 Foxg1-MCL-$1^{\Delta/\Delta}$ brains (Figure 7A), consistent with our previous immunohistochemistry results (Arbour *et al*, 2008). However, LC3 lipidation (LC3-II) and p62 levels were similar between heterozygous and knockout mice (Figure 7A). To further characterise the autophagic response of Foxg1-MCL-$1^{\Delta/\Delta}$ mice, E15.5 embryos were stained for endogenous LC3 and analysed by fluorescence microscopy. As shown in Figure 7B, no major differences in LC3 staining were observed in the ventricular zone (VZ) between control and MCL-1(Foxg1)$^{\Delta/\Delta}$ embryos (Figure 7B; top panels, VZ). However, there was a striking increase in LC3 staining in the cortical plate (where post-mitotic neurons reside) of control embryos (Figure 7B; middle left panel). A similar increase in LC3 staining was seen in MCL-1(Foxg1)$^{\Delta/\Delta}$ embryos, although, as previously reported (Arbour *et al*, 2008), the cortex was much smaller (Figure 7B; middle right panel). As the percentage of LC3 vesicles that

 

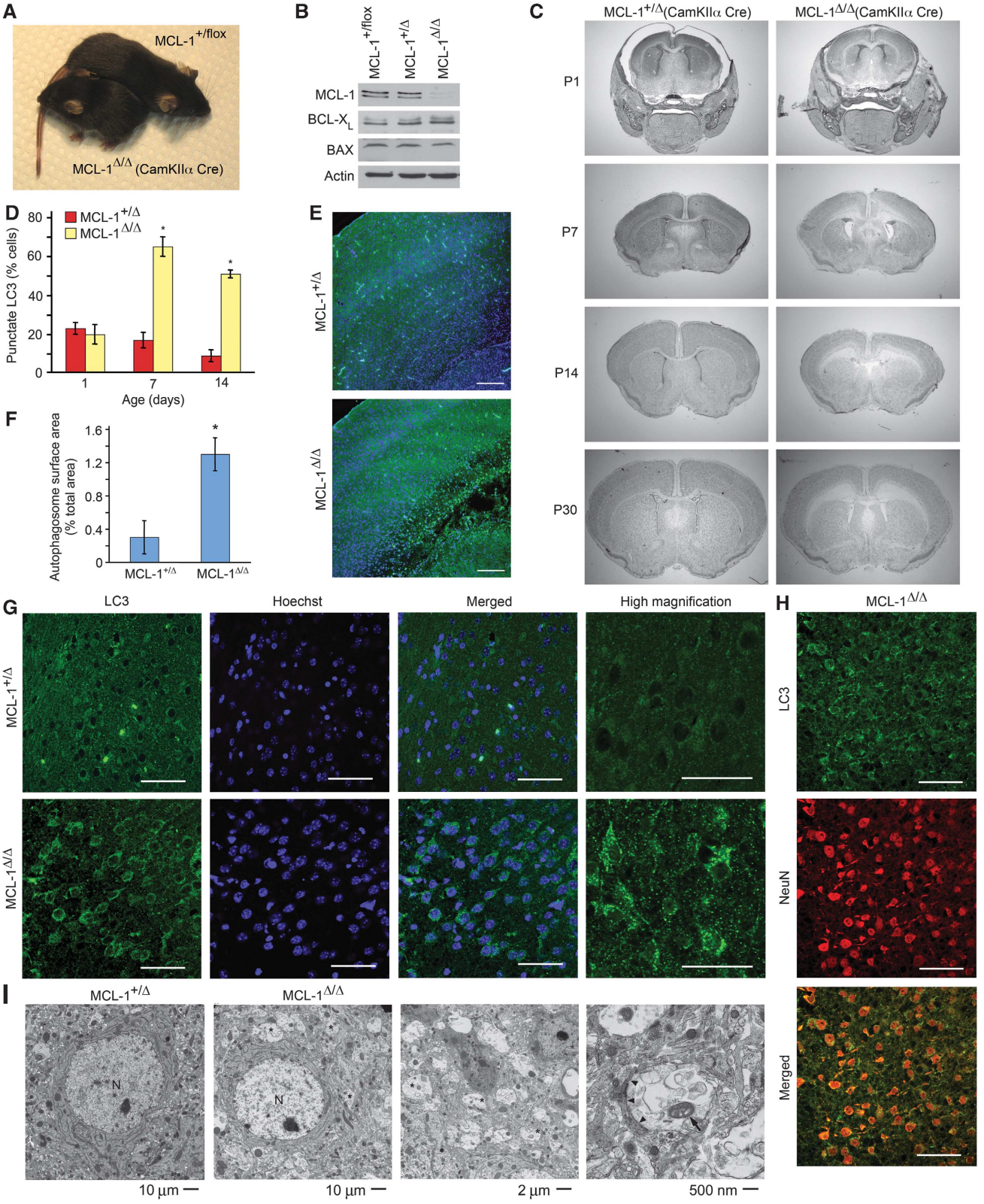


**Figure 5** Conditional knockout of MCL-1 in the forebrain activates an exacerbated autophagic response. (**A**) Control and MCL-1$^{\Delta/\Delta}$ mice. (**B**) Expression levels of various BCL-2 homologues in the cortices of animals of the indicated genotypes. (**C**) Brain morphology of MCL-1$^{\Delta/\Delta}$. Brain sections were stained with cresyl violet and imaged using a $\times 1$ objective. (**D**–**G**) Cortical neurons around the lesion in MCL-1$^{\Delta/\Delta}$ animals are positive for the autophagic marker LC3. Brain sections from animals with the indicated genotypes (P14 for **E**, **G**; P7 for **H**) were stained for LC3 (Green) and the neuronal marker NeuN (in **H**, red), along with the nuclear stain Hoechst (Blue). Confocal images were taken using $\times 10$ (**E**) or $\times 63$ (**G**, **H**) objectives. Scale bars = 200 μm (**E**); 50 μm (**G**, **H**). Quantification of the LC3 staining is shown in **D**. The total number of cells was determined by counting the Hoechst-positive nuclei. Data are expressed as percent of LC3-positive cells in at least three animals per genotype ± s.d. *$P<0.01$. (**F**) Quantification of the total surface area occupied by autophagosomes. Data are expressed as percent of total cortical area covered by autophagosomes in at least 16 EM images per genotype ± s.d. $P<0.005$ (**I**) Representative EM images from MCL-1$^{+/\Delta}$ and MCL-1$^{\Delta/\Delta}$ P14 mice. N, nucleus; *, autophagosomal structures; arrowheads, double membrane; arrow, mitochondrion inside a vesicle.

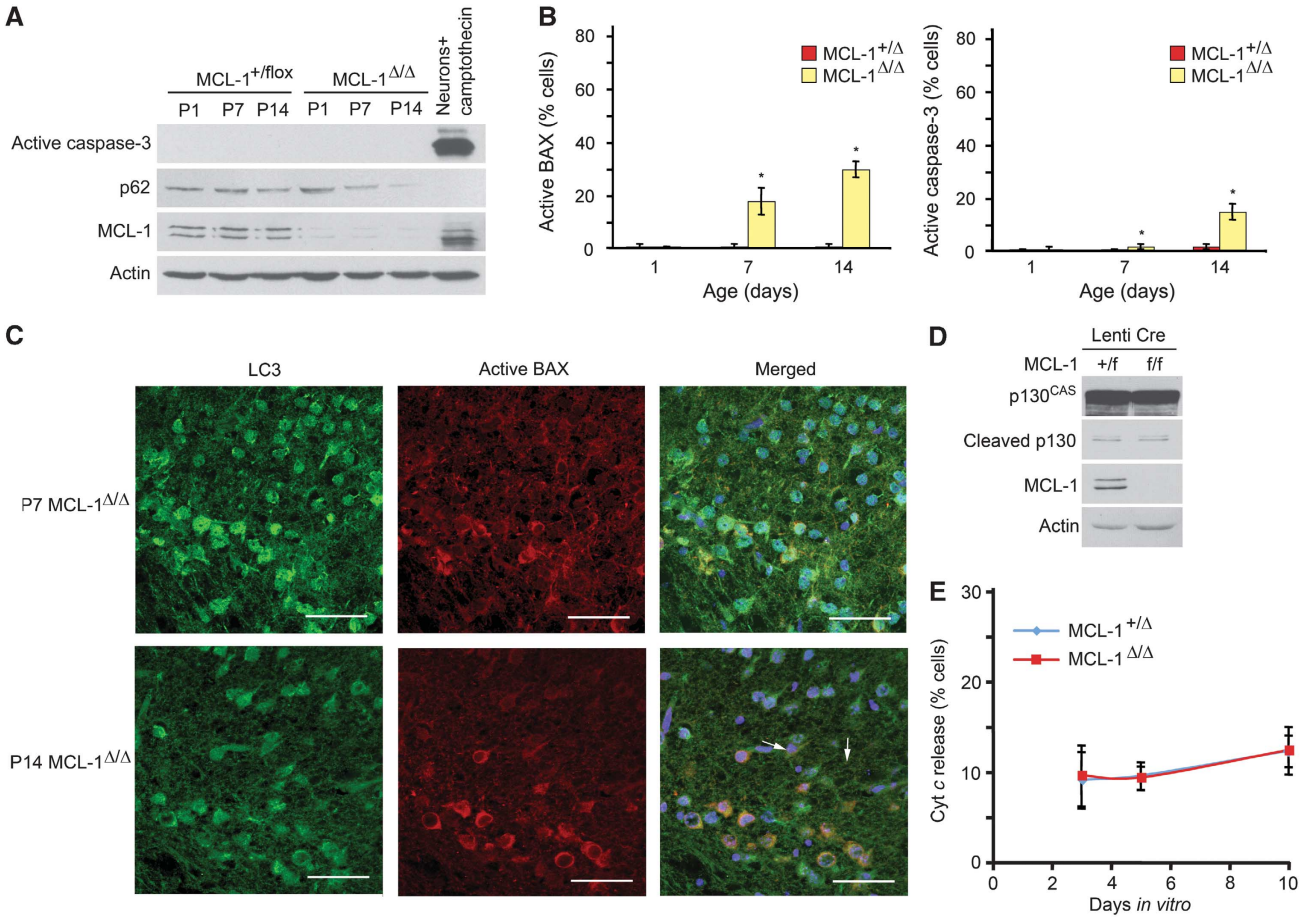


**Figure 6** Regulation of apoptosis in MCL-1 conditional knockout mice. (**A**) Cortices from the indicated genotypes and ages were analysed by western blot for the presence of active caspase-3, p62 and MCL-1. Primary cortical neurons treated for 12 h with camptothecin were used as a positive control for active caspase-3. (**B**) Active BAX (6A7) and active caspase-3 were also quantified by staining the cortex of 1- to 14-day-old MCL-$1^{\Delta/\Delta}$ mice. Representative images from at least three sections from each animal were counted. The total number of cells was determined by counting the Hoechst-positive nuclei. Data are expressed as percent of positive cells for at least three animals per genotype ± s.d. $^*P<0.05$. (**C**) Active BAX is present in a subset of LC3-positive cells. Sections from P7 and P14 MCL-$1^{\Delta/\Delta}$ brains were stained for LC3 (Green) and active BAX (6A7; Red). Confocal images were taken using × 63 objective. Arrows point to BAX-positive, LC3-negative cells. Representative images are shown. Scale bars = 50 μm. (**D**) Primary cortical neurons of the indicated genotypes were infected with a lentivirus expressing Cre at the time of plating and analysed for the presence of the caspase-cleaved fragment of the caspase-3 substrate $p130^{CAS}$ 5 days later. Alternatively (**E**), the neurons were analysed for cytochrome *c* release by immunofluorescence. Data are expressed as percent of positive cells for at least three embryos per genotype ± s.d.

colocalised with the lysosomal marker LAMP1 did not differ between the cortex and the VZ (Figure 7C), these results suggest that the autophagic machinery is upregulated as neurons differentiate, consistent with the autophagic response observed in MCL-$1^{\Delta/\Delta}$ neurons.

To determine whether post-mitotic neurons and neural progenitors express a different complement of apoptotic and autophagic genes, cortical neurons and neurospheres (neural progenitors) were cultured from E14.5 embryos. There was a marked difference in the expression of proapoptotic and autophagy-related proteins between progenitors and post-mitotic neurons (Figure 7D). For example, expression of the BH3-only proteins BIM and Puma was higher in neurospheres. Conversely, ATG7 and the ATG5–ATG12 conjugate, two important autophagy regulatory proteins, were expressed at higher levels in neurons (Figure 7D). This suggests that autophagy and apoptosis are differentially regulated as neurons differentiate, consistent with the pattern of LC3 staining observed in E15.5 embryos. As a control, the purity of the cultures was assessed by blotting for the neuronal marker Tuj-1 and the progenitor marker Nestin (Figure 7D). As BH3-only proteins are required for BAX activation, a key step in determining cell fate downstream of MCL-1 degradation (Figure 1), these differences suggest that neural progenitors have a higher propensity than neurons to undergo apoptosis under low-nutrient conditions. This was tested by measuring apoptosis and autophagy in EBSS-treated neurospheres and neurons. We first verified that starvation caused MCL-1 degradation in neurospheres (Figure 7E). While both neurons and neurospheres had increased LC3-II levels following induction of autophagy, only neurospheres showed an increase in apoptosis, as evaluated by $p130^{CAS}$ cleavage and cytochrome *c* release (Figure 7F and G). This indicates that neural progenitors are more susceptible than neurons to apoptosis following nutrient deprivation.

### *Inhibition of autophagy activates apoptosis in CamKIIα Cre MCL-1 knockout*

Altogether, these results indicate that neurons, as long-lived post-mitotic cells, preferentially respond to stress by

 

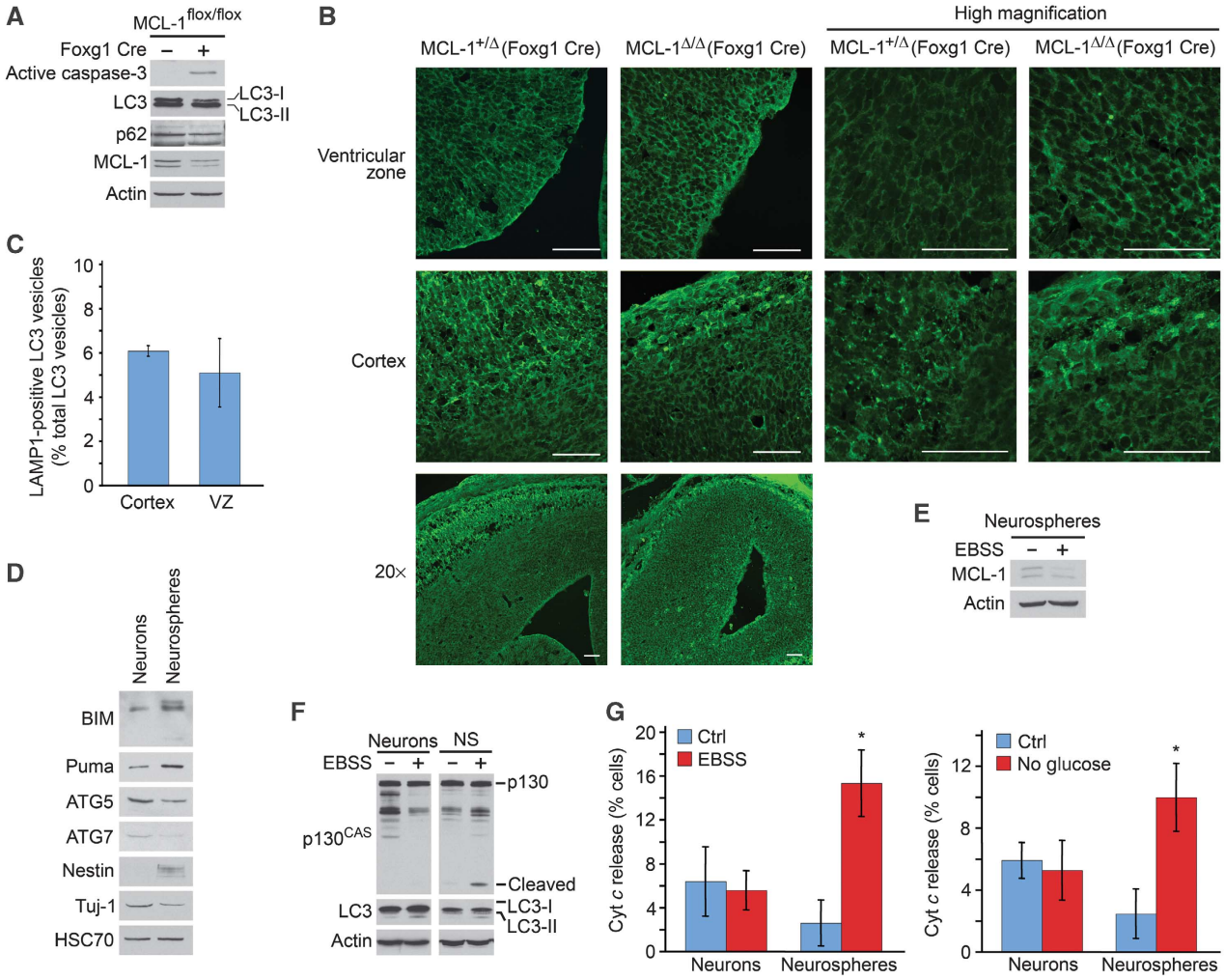


**Figure 7** Apoptosis and autophagy are activated in a developmentally regulated manner in MCL-1-null animals. (**A**) Brains from E12.5 Foxg1 Cre MCL-1 animals were analysed by western blot for the presence of the caspase-cleaved fragment of the caspase-3 substrate $p130^{CAS}$ and the autophagic markers LC3 and p62. (**B**) Autophagy in Foxg1 Cre MCL-$1^{\Delta/\Delta}$ mice. Brain sections from E15.5 animals with the indicated genotypes were stained for LC3 (green). Confocal images were taken using ×20 (bottom panel) or ×63 (top and middle panels) objectives. Scale bars = 50 μm. (**C**) Colocalization of LC3 vesicles with the lysosomal marker LAMP1 was analysed by immunohistochemistry in E15.5 wild-type embryos. Data are expressed as the percentage of LC3 vesicles that are LAMP1-positive ± s.d. About 100 LC3 vesicles were counted per section, with four sections per embryo. VZ, ventricular zone. (**D**) Primary cortical neurons and neuronal progenitor cells were analysed for the presence of the indicated apoptosis (BIM, Puma) and autophagy (ATG7, ATG5-ATG12) related proteins as well as Tuj-1 (neuronal marker), Nestin (neural progenitor marker) and HSC70 (loading control). (**E**) Primary neurospheres were treated for 8 h with EBSS and analysed by western blot for the presence of MCL-1 and actin as a loading control. (**F**) Primary neurons and neurospheres were treated as in **E** and analysed by western blot for $p130^{CAS}$, LC3 and actin as a loading control. Alternatively, they were analysed by immunofluorescence for cytochrome *c* release (**G**) in the presence of 50 μM zVAD-FMK to prevent apoptotic cells from detaching from the coverslip. Data are expressed as the average of 3–7 embryos ± s.d. $^*P<0.001$.

activating autophagy rather than apoptosis, in an attempt to restore homeostasis. Thus, inhibiting autophagy in neurons should drive these cells towards an apoptotic response. To test this hypothesis, MCL-$1^{\Delta/\Delta}$ mice were crossed with mice deficient for Beclin-1, as it is an essential autophagy protein regulated by MCL-1 (Figure 4; Maiuri *et al*, 2007a). As homozygous deletion of Beclin-1 is embryonically lethal, we examined Beclin-$1^{+/-}$ animals, which have a 30–50% reduction in autophagy (Qu *et al*, 2003; Yue *et al*, 2003). MCL-$1^{\Delta/\Delta}$ Beclin-$1^{+/-}$ mice were born at the expected ratio, but started to die around 2 weeks of age (Figure 8E). MCL-$1^{\Delta/\Delta}$ Beclin-$1^{+/-}$ mice had a reduced lifespan compared with their MCL-$1^{\Delta/\Delta}$ Beclin-$1^{+/+}$ littermates (median lifespan of 21 days for the former, compared with 49 days the latter). Nevertheless, as with MCL-$1^{\Delta/\Delta}$ mice, some MCL-$1^{\Delta/\Delta}$ Beclin$^{+/-}$ animals lived to 3 months of age. However, cresyl violet staining of brain sections did not reveal major differences in morphology between MCL-$1^{\Delta/\Delta}$ and MCL-$1^{\Delta/\Delta}$ Beclin$^{+/-}$ brains (Figure 8A).

To determine the extent of apoptosis, brain sections from each genotype were stained for active BAX (6A7) and active caspase-3. The number of cells positive for active BAX and active caspase-3 was significantly increased in MCL-$1^{\Delta/\Delta}$ Beclin-$1^{+/-}$ sections compared with MCL-$1^{\Delta/\Delta}$ Beclin-$1^{+/+}$ (Figure 8B and C). Moreover, the number of 6A7-positive, LC3-negative cells was doubled in MCL-$1^{\Delta/\Delta}$ Beclin-$1^{+/-}$ mice compared with MCL-$1^{\Delta/\Delta}$ (Figure 8D). This suggests that a greater proportion of neurons activate apoptosis when

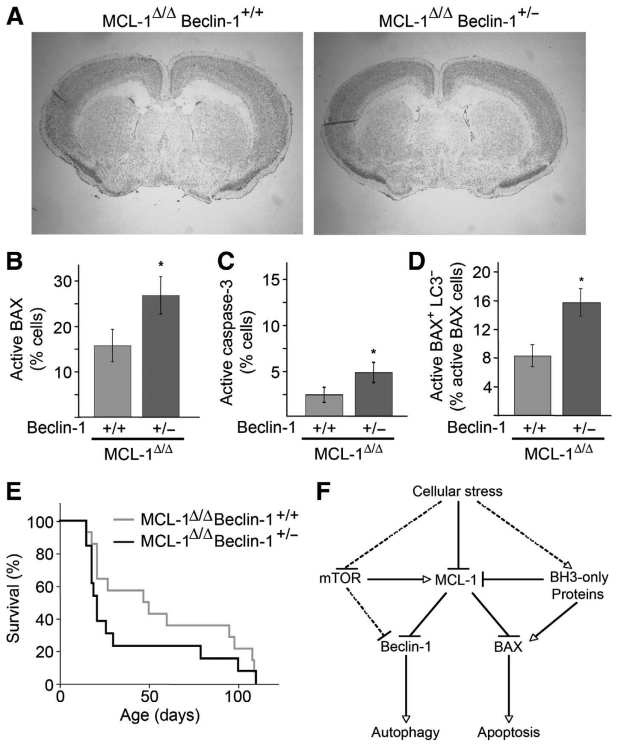


**Figure 8** Inhibition of autophagy in MCL-1-deficient neurons activates apoptosis. (**A**) Brain morphology of P14 MCL-$1^{\Delta/\Delta}$ Beclin-$1^{+/-}$ mice. Brain sections were stained with cresyl violet and imaged using a $\times 1$ objective. (**B**–**D**) Active BAX (6A7; **B**) and active caspase-3 (**C**) were quantified by staining the cortex of 14-day-old MCL-$1^{\Delta/\Delta}$ and MCL-$1^{\Delta/\Delta}$ Beclin-$1^{+/-}$ mice. The number of BAX-positive LC3-negative cells was also quantified. (**D**) Representative images from at least three sections from each animal were counted. The total number of cells was determined by counting the Hoechst-positive nuclei. Data are expressed as percent of positive cells for least three animals per genotype ± s.d. $^*P<0.05$. (**E**) Survival data from MCL-$1^{\Delta/\Delta}$ ($n=14$) and their MCL-$1^{\Delta/\Delta}$ Beclin-$1^{+/-}$ littermates ($n=13$). (**F**) Model for the role of MCL-1 in regulating both autophagy and apoptosis. See text for details.

Beclin-1 levels are reduced, consistent with previous reports on the relationship between apoptosis and autophagy in stressed cells in culture (Boya *et al*, 2005; Luo and Rubinsztein, 2010). Altogether, our results suggest that MCL-1 functions as an upstream regulator of a stress–response pathway controlling both apoptosis and autophagy in a developmentally regulated manner.

## Discussion

Apoptosis is a critical process regulating development of multicellular organisms. However, while neural precursors readily induce apoptosis following stress, neurons are more resistant and use autophagy as a mechanism to dispose of damaged cellular components. This context-dependent regulation of apoptosis and autophagy is controlled by MCL-1, an antiapoptotic BCL-2 homologue with a very short half-life. In fact, we show here that MCL-1 levels regulate autophagy, both in cells in culture and in post-mitotic neurons.

Deletion of MCL-1 in several systems, including haematopoietic precursors, liver and neuronal progenitors, leads to activation of apoptosis, resulting in cellular loss (Opferman *et al*, 2003, 2005; Arbour *et al*, 2008; Weber *et al*, 2010). In contrast, we show here that autophagy is an important cellular outcome following deletion of MCL-1 in post-mitotic neurons. This is supported by the observation that virtually all neurons (stained with NeuN) are positive for LC3 in P7 mice (Figure 5H), while all BAX-positive cells are also LC3-positive at that age (Figure 6C). In addition, *in vitro* deletion of MCL-1, a setting in which apoptotic cells are not rapidly removed, did not induce any apoptosis in cortical neurons over wild-type levels, even after 10 days (Figure 6D and E). These data support our interpretation that MCL-1 deficiency induces a robust autophagic response in mature neurons.

The outcome of the deletion of MCL-1 in neuronal precursors and post-mitotic neurons also supports a model in which MCL-1 coordinately regulates apoptosis and autophagy in a context-dependent manner. For example, post-mitotic neurons display a greater amount of autophagy-related proteins and primarily activate autophagy when starved. In contrast, a portion of neural precursors, which express higher levels of proapoptotic proteins than neurons, activate apoptosis in response to the same stress. The relationship between apoptosis and autophagy is however complex, as autophagy deficiency renders cells more susceptible to apoptosis while apoptosis inhibits autophagy (Boya *et al*, 2005; Luo and Rubinsztein, 2010). In that context, it is noteworthy that MCL-1 knockout neurons could be forced to undergo apoptosis by decreasing the levels of the autophagy regulator Beclin-1. Conversely, tBID-dependent activation of BAX in starved HeLa cells pushed these cells towards apoptosis. On the basis of these findings, we propose the following model for the coordinated regulation of apoptosis and autophagy by MCL-1 (Figure 8F). Cellular stress causes the degradation of MCL-1, relieving its inhibitory effect on both autophagy (Beclin-1) and apoptosis (BAX). However, other signals are required for complete activation of either pathway. These additional autophagy or apoptosis-specific signalling pathways become activated by cellular stress, as a consequence of both the nature of the stress and the cellular context. Of note, MCL-1 localises to mitochondria where it interacts with Beclin-1, whereas BCL-2 functionally interacts with Beclin-1 at the ER. Given that both ER (Axe *et al*, 2008) and mitochondria (Hailey *et al*, 2010) have recently been suggested to provide lipids for autophagosome formation, MCL-1 could be required to regulate the mitochondrial pathway of autophagosome formation.

Regulation of the balance between autophagy and apoptosis is critical during development, as both processes have an important role. For example, deletion of the autophagy regulator Ambra-1 causes unbalanced cell proliferation and excessive apoptotic cell death during neuronal development, leading to severe neural tube defects (Fimia *et al*, 2007). On the other hand, deletion of key components of the mitochondrial pathway of apoptosis results in brain overgrowth (reviewed in Ranger *et al* (2001)). In addition, the regulation of both processes has a crucial role in the outcome of several pathological conditions, such as neurodegenerative diseases and cancer. In the case of neurodegenerative diseases, while maintaining a basal level of autophagy to dispose of damaged organelles or proteins is critical for survival, strong induction of autophagy could lead to cell death (Germain and Slack, 2010). This could potentially be as a consequence of the clearance of mitochondria or other

 

organelles (Xue *et al*, 2001) or, as our results suggest in the case of MCL-1, because sustained activation of autophagy activates an apoptotic response.

Several pathways have previously been shown to cause MCL-1 degradation. First, the ubiquitin ligases Mule and ßTRCP ubquitinate MCL-1 and promote its degradation (Warr *et al*, 2005; Zhong *et al*, 2005; Maurer *et al*, 2006; Ding *et al*, 2007). Interestingly, MCL-1 degradation caused by serum withdrawal is the consequence of GSK3-dependent recruitment of ßTRCP (Ding *et al*, 2007). Ubiquitination of MCL-1 by these two E3 ligases has, however, been linked to apoptosis. More recently, MCL-1 transcription has been shown to be regulated by mTOR, the key regulator of transcription that is inactivated following nutrient starvation (Mills *et al*, 2008; Pradelli *et al*, 2010). It is thus likely that MCL-1 degradation following nutrient starvation is the direct consequence of mTOR inhibition, as recently suggested. In any case, the position of MCL-1 as an upstream stress-sensitive protein coordinately regulating apoptosis and autophagy renders MCL-1 a key regulator of cell fate under stress conditions.

## Materials and methods

### *Cell culture, transfections and infections*

H1299 cells stably expressing GFP–LC3 (gift from Dr Gordon Shore, McGill University), HeLa cells and MEFs were cultured in Dulbecco's modified Eagle's medium (DMEM) supplemented with 10% fetal bovine serum. For the induction of autophagy, cells were washed in PBS and incubated for the indicated time in either EBSS(Sigma) or DMEM, containing no glucose or pyruvate supplemented with 10% fetal bovine serum. Where indicated, cells were pre-treated 1 h with 3MA (5 mM) or Bafilomycin (200 nM) before inducing autophagy. Infections with an adenoviral vector coding for myc-tagged MCL-1 or HA-tBID (gift from Gordon Shore) were carried out as described (Germain *et al*, 2005). For the siRNA experiments, cells were transfected with 50 nM Ctrl or MCL-1 siRNA (Santa Cruz Biotechnology) using SilentFect (Bio-Rad Laboratories) and analysed after 24 h. Subcelular fractionation was carried as described (Germain *et al*, 2002).

Neurospheres, cortical neurons and CGNs were cultured as described previously (Cregan *et al*, 1999; Fortin *et al*, 2001; Vanderluit *et al*, 2004). For immunofluorescence, neurosphere were grown on coverslips for 2 days in neurobasal containing 0.5 mM L-glutamine, 1% N2 supplement, 2% B27 supplement, 10 ng/ml bFGF and 20 ng/ml EGF. Where indicated, neurons were infected at the time of plating with a lentiviral vector expressing the Cre recombinase using an MOI of 2. Hypoxic cell death was induced using a humidified environmental chamber (Coy Laboratory, Grass Lake, MI) set at 37°C. Oxygen concentration was maintained at 1% with a calibrated gas mixture of 95% nitrogen and 5% carbon dioxide. CGN cultures were treated with 10 μM cytosine–arabinoside after 2 days *in vitro* to inhibit glial growth, and incubated in the chamber after 7–8 days *in vitro* for 16–18 h at 1% oxygen in the presence of the NMDA receptor blocker, MK801 (10 μM). Cultures were then allowed to reoxygenate by incubating under normoxic conditions at 37°C. Cells were collected at the indicated times following reoxygenation.

### *Antibodies and immunoblots*

The following antibodies were used: mouse anti-mtHSP70 (ABR Bioreagents); mouse anti-HSC70 (Abcam); mouse anti-Tuj-1 (Gift from Dr Dave Brown); mouse anti-Nestin (Research Diagnostics Inc.); guinea-pig anti p62 (Progen Biotechnik); rabbit anti-mouse MCL-1 (Rockland Immunochemicals); rat anti-APAF-1 and mouse anti-NeuN (Chemicon); rabbit anti-human MCL-1, mouse anti-human p62, rabbit anti-mouse p62, rabbit anti-Beclin-1, rabbit anti-ATG-7, mouse anti-BCL-X, mouse anti-human LAMP1 and rabbit anti-BAX (Santa Cruz Biotechnology); mouse anti-GFP (Clonetech), mouse anti-actin (Sigma); rabbit anti-LC3 and rabbit anti-ATG5 (Novus Biologicals); mouse anti-mouse p62, mouse anti-cytochrome *c*, rabbit anti-BIM, mouse anti-BCL-2, mouse anti-active BAX (6A7), mouse anti-calreticulin (BD Pharmingen); rabbit anti-BAK (Upstate); rabbit anti-BCL-W, rabbit anti-HA, rabbit anti-PUMA and rabbit anti-active caspase-3 (Cell Signaling Technology). Cells were lysed in 10 mM Tris–HCl, pH 7.9, 150 mM NaCl, 1 mM EDTA, 1% Triton X-100 supplemented with a protease inhibitor mixture (Sigma-Aldrich). For immunoprecipitation, lysates were incubated for 2 h with the antibody and precipitated with protein G-Sepharose. For immunoblot analysis, proteins were subjected to SDS–PAGE, transferred to nitrocellulose membranes, and blotted with specific antibodies. Blots were incubated with horseradish peroxidase-conjugated secondary antibodies and visualised by enhanced chemiluminescence (Amersham Biosciences).

### *Immunofluorescence*

For immunofluorescence, cells were grown on coverslips and treated as indicated in the figure legends. Cells were then fixed with 4% paraformaldehyde (PFA) and analysed by immunofluorescence using AlexaFluor secondary antibodies (Molecular Probes). All images were taken using a Zeiss 510 meta confocal microscope. Quantification of GFP–LC3 staining was performed by calculating the surface area of the GFP–LC3 fluorescence above a set threshold (that was kept constant throughout the experiments) over the total surface area of the cell, using the Image J software.

### *Animals*

All experiments were approved by the University of Ottawa's Animal Care Ethics Committee adhering to the Guidelines of the Canadian Council on Animal Care. To generate forebrain-specific MCL-1 KO mice, the previously described floxed MCL-1 mice were crossed with CamKIIα Cre mice (Casanova *et al*, 2001). MCL-1 mice were also crossed with Beclin-1$^{+/-}$ mice (gift from Dr Beth Levine). All mice were kept on a C57Bl/6 background. Animals were genotyped according to standard protocols with previously published primers for MCL-1 Beclin-1 and Cre.

### *Tissue processing and immunohistochemistry*

Mice were euthanised with a lethal injection of sodium pentobarbitol. For immunohistochemistry, mice were perfused with 1 × PBS followed by cold 4% PFA. Brains were then removed, post-fixed overnight in 4% PFA, cryoprotected in 20% sucrose in 1 × PBS, and frozen. Sections were collected as 14 μm coronal cryosections on Superfrost Plus® slides (Fisher Scientific). For western blot analysis, brains were removed, cortices dissected and flash-frozen in liquid nitrogen. For EM, mice were perfused with a combination of 2% PFA and 2% glutaraldehyde. Pieces of cortex not $>1\,mm^2$ were taken and processed as described (Cheung *et al*, 2006).

### *Statistical analysis*

Statistical differences were determined using Student's *t*-test or one-way ANOVA. $P<0.05$ was considered statistically significant.

## Acknowledgements

We thank Peter Rippstein for performing the electron microscopy, Jason MacLaurin and Cathy Tsilfidis for the generation of viral vectors, Linda Jiu for tissue preparation and Lisa Julian for help with the neurosphere cultures. We also thank Heidi McBride, Melissa Kelly, Renaud Vandenbosch, Mireille Khacho and Jennifer Michel for their insightful comments on the manuscript. This work was supported by a grant from the Heart and Stroke Foundation of Canada to RSS. MG is the recipient of research fellowships from the Heart and Stroke Foundation of Canada and Parkinson's Society of Canada.

## Conflict of interest

The authors declare that they have no conflict of interest.

## References

Arbour N, Vanderluit JL, Le Grand JN, Jahani-Asl A, Ruzhynsky VA, Cheung EC, Kelly MA, MacKenzie AE, Park DS, Opferman JT, Slack RS (2008) Mcl-1 is a key regulator of apoptosis during CNS development and after DNA damage. *J Neurosci* **28:** 6068–6078

Axe EL, Walker SA, Manifava M, Chandra P, Roderick HL, Habermann A, Griffiths G, Ktistakis NT (2008) Autophagosome formation from membrane compartments enriched in phosphatidylinositol 3-phosphate and dynamically connected to the endoplasmic reticulum. *J Cell Biol* **182:** 685–701

Boya P, Gonzalez-Polo RA, Casares N, Perfettini JL, Dessen P, Larochette N, Metivier D, Meley D, Souquere S, Yoshimori T, Pierron G, Codogno P, Kroemer G (2005) Inhibition of macroautophagy triggers apoptosis. *Mol Cell Biol* **25:** 1025–1040

Casanova E, Fehsenfeld S, Mantamadiotis T, Lemberger T, Greiner E, Stewart AF, Schutz G (2001) A CamKIIalpha iCre BAC allows brain-specific gene inactivation. *Genesis* **31:** 37–42

Chang NC, Nguyen M, Germain M, Shore GC (2010) Antagonism of Beclin 1-dependent autophagy by BCL-2 at the endoplasmic reticulum requires NAF-1. *EMBO J* **29:** 606–618

Cheung EC, Joza N, Steenaart NA, McClellan KA, Neuspiel M, McNamara S, MacLaurin JG, Rippstein P, Park DS, Shore GC, McBride HM, Penninger JM, Slack RS (2006) Dissociating the dual roles of apoptosis-inducing factor in maintaining mitochondrial structure and apoptosis. *EMBO J* **25:** 4061–4073

Chou CH, Lee RS, Yang-Yen HF (2006) An internal EELD domain facilitates mitochondrial targeting of Mcl-1 via a Tom70-dependent pathway. *Mol Biol Cell* **17:** 3952–3963

Cregan SP, MacLaurin JG, Craig CG, Robertson GS, Nicholson DW, Park DS, Slack RS (1999) Bax-dependent caspase-3 activation is a key determinant in p53-induced apoptosis in neurons. *J Neurosci* **19:** 7860–7869

Ding Q, He X, Hsu JM, Xia W, Chen CT, Li LY, Lee DF, Liu JC, Zhong Q, Wang X, Hung MC (2007) Degradation of Mcl-1 by beta-TrCP mediates glycogen synthase kinase 3-induced tumor suppression and chemosensitization. *Mol Cell Biol* **27:** 4006–4017

Erlich S, Mizrachy L, Segev O, Lindenboim L, Zmira O, Adi-Harel S, Hirsch JA, Stein R, Pinkas-Kramarski R (2007) Differential interactions between Beclin 1 and Bcl-2 family members. *Autophagy* **3:** 561–568

Fimia GM, Stoykova A, Romagnoli A, Giunta L, Di Bartolomeo S, Nardacci R, Corazzari M, Fuoco C, Ucar A, Schwartz P, Gruss P, Piacentini M, Chowdhury K, Cecconi F (2007) Ambra1 regulates autophagy and development of the nervous system. *Nature* **447:** 1121–1125

Fortin A, Cregan SP, MacLaurin JG, Kushwaha N, Hickman ES, Thompson CS, Hakim A, Albert PR, Cecconi F, Helin K, Park DS, Slack RS (2001) APAF1 is a key transcriptional target for p53 in the regulation of neuronal cell death. *J Cell Biol* **155:** 207–216

Germain M, Duronio V (2007) The N terminus of the anti-apoptotic BCL-2 homologue MCL-1 regulates its localization and function. *J Biol Chem* **282:** 32233–32242

Germain M, Mathai JP, McBride HM, Shore GC (2005) Endoplasmic reticulum BIK initiates DRP1-regulated remodelling of mitochondrial cristae during apoptosis. *EMBO J* **24:** 1546–1556

Germain M, Mathai JP, Shore GC (2002) BH-3-only BIK functions at the endoplasmic reticulum to stimulate cytochrome *c* release from mitochondria. *J Biol Chem* **277:** 18053–18060

Germain M, Slack RS (2010) Dining in with BCL-2: new guests at the autophagy table. *Clin Sci (Lond)* **118:** 173–181

Hailey DW, Rambold AS, Satpute-Krishnan P, Mitra K, Sougrat R, Kim PK, Lippincott-Schwartz J (2010) Mitochondria supply membranes for autophagosome biogenesis during starvation. *Cell* **141:** 656–667

Hara T, Nakamura K, Matsui M, Yamamoto A, Nakahara Y, Suzuki-Migishima R, Yokoyama M, Mishima K, Saito I, Okano H, Mizushima N (2006) Suppression of basal autophagy in neural cells causes neurodegenerative disease in mice. *Nature* **441:** 885–889

He C, Klionsky DJ (2009) Regulation mechanisms and signaling pathways of autophagy. *Annu Rev Genet* **43:** 67–93

Klionsky DJ, Abeliovich H, Agostinis P, Agrawal DK, Aliev G, Askew DS, Baba M, Baehrecke EH, Bahr BA, Ballabio A, Bamber BA, Bassham DC, Bergamini E, Bi X, Biard-Piechaczyk M, Blum JS, Bredesen DE, Brodsky JL, Brumell JH, Brunk UT *et al* (2008) Guidelines for the use and interpretation of assays for monitoring autophagy in higher eukaryotes. *Autophagy* **4:** 151–175

Komatsu M, Waguri S, Chiba T, Murata S, Iwata J, Tanida I, Ueno T, Koike M, Uchiyama Y, Kominami E, Tanaka K (2006) Loss of autophagy in the central nervous system causes neurodegeneration in mice. *Nature* **441:** 880–884

Kook S, Shim SR, Choi SJ, Ahnn J, Kim JI, Eom SH, Jung YK, Paik SG, Song WK (2000) Caspase-mediated cleavage of p130cas in etoposide-induced apoptotic Rat-1 cells. *Mol Biol Cell* **11:** 929–939

Luo S, Rubinsztein DC (2010) Apoptosis blocks Beclin 1-dependent autophagosome synthesis: an effect rescued by Bcl-xL. *Cell Death Differ* **17:** 268–277

Maiuri MC, Le Toumelin G, Criollo A, Rain JC, Gautier F, Juin P, Tasdemir E, Pierron G, Troulinaki K, Tavernarakis N, Hickman JA, Geneste O, Kroemer G (2007a) Functional and physical interaction between Bcl-X(L) and a BH3-like domain in Beclin-1. *EMBO J* **26:** 2527–2539

Maiuri MC, Zalckvar E, Kimchi A, Kroemer G (2007b) Self-eating and self-killing: crosstalk between autophagy and apoptosis. *Nat Rev Mol Cell Biol* **8:** 741–752

Martin AP, Mitchell C, Rahmani M, Nephew KP, Grant S, Dent P (2009) Inhibition of MCL-1 enhances lapatinib toxicity and overcomes lapatinib resistance via BAK-dependent autophagy. *Cancer Biol Ther* **8:** 2084–2096

Maurer U, Charvet C, Wagman AS, Dejardin E, Green DR (2006) Glycogen synthase kinase-3 regulates mitochondrial outer membrane permeabilization and apoptosis by destabilization of MCL-1. *Mol Cell* **21:** 749–760

Mehrpour M, Esclatine A, Beau I, Codogno P (2010) Overview of macroautophagy regulation in mammalian cells. *Cell Res* **20:** 748–762

Mills JR, Hippo Y, Robert F, Chen SM, Malina A, Lin CJ, Trojahn U, Wendel HG, Charest A, Bronson RT, Kogan SC, Nadon R, Housman DE, Lowe SW, Pelletier J (2008) mTORC1 promotes survival through translational control of Mcl-1. *Proc Natl Acad Sci USA* **105:** 10853–10858

Nijhawan D, Fang M, Traer E, Zhong Q, Gao W, Du F, Wang X (2003) Elimination of Mcl-1 is required for the initiation of apoptosis following ultraviolet irradiation. *Genes Dev* **17:** 1475–1486

Opferman JT, Iwasaki H, Ong CC, Suh H, Mizuno S, Akashi K, Korsmeyer SJ (2005) Obligate role of anti-apoptotic MCL-1 in the survival of hematopoietic stem cells. *Science* **307:** 1101–1104

Opferman JT, Letai A, Beard C, Sorcinelli MD, Ong CC, Korsmeyer SJ (2003) Development and maintenance of B and T lymphocytes requires antiapoptotic MCL-1. *Nature* **426:** 671–676

Pattingre S, Tassa A, Qu X, Garuti R, Liang XH, Mizushima N, Packer M, Schneider MD, Levine B (2005) Bcl-2 antiapoptotic proteins inhibit Beclin 1-dependent autophagy. *Cell* **122:** 927–939

Pickford F, Masliah E, Britschgi M, Lucin K, Narasimhan R, Jaeger PA, Small S, Spencer B, Rockenstein E, Levine B, Wyss-Coray T (2008) The autophagy-related protein beclin 1 shows reduced expression in early Alzheimer disease and regulates amyloid beta accumulation in mice. *J Clin Invest* **118:** 2190–2199

Pradelli LA, Beneteau M, Chauvin C, Jacquin MA, Marchetti S, Munoz-Pinedo C, Auberger P, Pende M, Ricci JE (2010) Glycolysis inhibition sensitizes tumor cells to death receptors-induced apoptosis by AMP kinase activation leading to Mcl-1 block in translation. *Oncogene* **29:** 1641–1652

Qu X, Yu J, Bhagat G, Furuya N, Hibshoosh H, Troxel A, Rosen J, Eskelinen EL, Mizushima N, Ohsumi Y, Cattoretti G, Levine B (2003) Promotion of tumorigenesis by heterozygous disruption of the beclin 1 autophagy gene. *J Clin Invest* **112:** 1809–1820

Ranger AM, Malynn BA, Korsmeyer SJ (2001) Mouse models of cell death. *Nat Genet* **28:** 113–118

Ravikumar B, Vacher C, Berger Z, Davies JE, Luo S, Oroz LG, Scaravilli F, Easton DF, Duden R, O'Kane CJ, Rubinsztein DC (2004) Inhibition of mTOR induces autophagy and reduces toxicity of polyglutamine expansions in fly and mouse models of Huntington disease. *Nat Genet* **36:** 585–595

Shibata M, Lu T, Furuya T, Degterev A, Mizushima N, Yoshimori T, MacDonald M, Yankner B, Yuan J (2006) Regulation of intracellular accumulation of mutant Huntingtin by Beclin 1. *J Biol Chem* **281:** 14474–14485

Spencer B, Potkar R, Trejo M, Rockenstein E, Patrick C, Gindi R, Adame A, Wyss-Coray T, Masliah E (2009) Beclin 1 gene transfer

 

activates autophagy and ameliorates the neurodegenerative pathology in alpha-synuclein models of Parkinson's and Lewy body diseases. *J Neurosci* **29:** 13578–13588

Vanderluit JL, Ferguson KL, Nikoletopoulou V, Parker M, Ruzhynsky V, Alexson T, McNamara SM, Park DS, Rudnicki M, Slack RS (2004) p107 regulates neural precursor cells in the mammalian brain. *J Cell Biol* **166:** 853–863

Warr MR, Acoca S, Liu Z, Germain M, Watson M, Blanchette M, Wing SS, Shore GC (2005) BH3-ligand regulates access of MCL-1 to its E3 ligase. *FEBS Lett* **579:** 5603–5608

Weber A, Boger R, Vick B, Urbanik T, Haybaeck J, Zoller S, Teufel A, Krammer PH, Opferman JT, Galle PR, Schuchmann M, Heikenwalder M, Schulze-Bergkamen H (2010) Hepatocyte-specific deletion of the antiapoptotic protein myeloid cell leukemia-1 triggers proliferation and hepatocarcinogenesis in mice. *Hepatology* **51:** 1226–1236

Xue L, Fletcher GC, Tolkovsky AM (2001) Mitochondria are selectively eliminated from eukaryotic cells after blockade of caspases during apoptosis. *Curr Biol* **11:** 361–365

Youle RJ, Strasser A (2008) The BCL-2 protein family: opposing activities that mediate cell death. *Nat Rev Mol Cell Biol* **9:** 47–59

Yue Z, Jin S, Yang C, Levine AJ, Heintz N (2003) Beclin 1, an autophagy gene essential for early embryonic development, is a haploinsufficient tumor suppressor. *Proc Natl Acad Sci USA* **100:** 15077–15082

Zhong Q, Gao W, Du F, Wang X (2005) Mule/ARF-BP1, a BH3-only E3 ubiquitin ligase, catalyzes the polyubiquitination of Mcl-1 and regulates apoptosis. *Cell* **121:** 1085–1095